Spring 2024

Kicking Up Dust on Utah's Off-Road Vehicle Trails: PI-SWERL Assessment of Anthropogenic Dust Emissions

Wyatt A. Wiebelhaus
University of South Dakota

KICKING UP DUST ON UTAH'S OFF-ROAD VEHICLE TRAILS: PI-SWERL ASSESSMENT OF ANTHROPOGENIC DUST EMISSIONS

by

Wyatt Wiebelhaus

A Thesis Submitted in Partial Fulfillment
Of the Requirements for the
University Honors Program

Department of Sustainability & Environment
The University of South Dakota
May 2024

The members of the Honors Thesis Committee appointed

to examine the thesis of Wyatt Wiebelhaus

find it satisfactory and recommend that it be accepted.

Mark Sweeney, Ph.D.

Professor of Sustainability & Environment

Director of the Committee

Brennan Jordan, Ph.D.

Professor of Sustainability & Environment

Jennifer Fierro, M.S.

Instructor of Sustainability & Environment

ABSTRACT

Kicking up dust on Utah's off-road vehicle trails: PI-SWERL assessment of anthropogenic dust emissions

Wyatt Wiebelhaus

Director: Mark Sweeney, Ph.D.

Upward trends in the use of off-highway vehicles (OHV) and the creation of new OHV trails facilitate an increase in soil disturbance and dust emissions in Utah. Anthropogenic destruction of soil crusts and the removal of vegetation by OHVs exposes soil and destroys soil structure, making the soil easier to erode by the wind. We used the PI-SWERL (Portable In Situ Wind Erosion Laboratory) to measure dust concentrations of disturbed and undisturbed soil. We tested soils at several popular OHV areas with landforms composed of sand dunes, playas, and Lake Bonneville sediments. Soil crust strength, grain size, and salinity were also measured. Dust emissions from undisturbed surfaces are low (~0.001 $mg/m^2/s$) in soils with high crust strength, vegetation, or high moisture content than those disturbed by OHVs. Disturbed OHV trails produced 1 to 5 orders of magnitude higher concentrations of dust (as high as 200 $mg/m^2/s$). Vegetation along with crusted surfaces protect soils from wind erosion. The generation of dust in Utah is multifaceted, likely owing a significant part of its production to the destruction of natural and crusted surfaces by anthropogenic activity.

KEYWORDS: Dust, Anthropogenic emissions, PI-SWERL, Utah, Off-road Vehicles

TABLE OF CONTENTS

LIST OF FIGURES

LIST OF TABLES

ACKNOWLEDGMENTS

This opportunity to conduct research at USD as an undergraduate student has become the highpoint of my college experience. This research has only been possible because of the opportunities and work put in by my advisor Mark Sweeney. I want to thank Mark for giving me the opportunity to learn firsthand about field research, and for being my thesis director. I also want to thank the Honors program and Melissa Berninger for helping push me academically to be the best student I can be and for advising me along the way.

I also want to thank the other crucial people during my time as a student such as: Jennifer Fierro, Brennan Jordan, and Sarah Chadima with the South Dakota Geologic Survey, for their guidance, patience, and support in my growth as a student and scientist as well as teaching me as much as they could in the time we spent together. This research was funded by a National Science Foundation grant EAR 2012082, and the South Dakota Space Grant Consortium.

Introduction

Human disturbance has accelerated the alteration and destruction of natural landforms, making them more likely to emit dust. Human modification of soils found within the arid drylands via land use change and land management in combination with aeolian processes often increases the level of dust produced (Goossens and Buck, 2009; Webb and Pierre, 2018; Duniway et al., 2019). Areas subjected to anthropogenic disturbance suffer from accelerated soil erosion and have an increased likelihood of producing a dust hazard to humans and the environment (Middleton, 2017). These dust areas are protected by several factors: natural biological soil crust (biocrust) (Fig 2D), physical soil crust formed due to high clay content and/or salt, and buffering by local vegetation cover increasing a surface's resistance to erosion (Rodriguez-Caballero et al., 2022).

Dust affects large areas of the Great Basin desert and increased aridity and disturbances coincide with observed annual cycles of dust storms in Utah (Hanenberger and Nicoll 2012; Nicoll et al., 2020). These seasonal events primarily occur during the summer months created by strong cyclonic systems pushing southwesterly winds into the eastern Great Basin (Hanenberger and Nicoll 2012). Continued drought and anthropogenic disturbance increase the likelihood of dangerous dust events in Utah affecting high population areas like Salt Lake City (Alberty and Mims, 2015; Walker et al. 2015). Dust storms also affect snowpack accelerating snow melt and lessening snow cover by up to a month (Painter et al., 2010). This acceleration of snow melt creates a positive feedback loop by decreasing the albedo, or reflectivity, of the snow making it absorb more heat from the sun thus melting faster (Lang et al., 2023).

Anthropogenically disturbed areas are more susceptible to wind erosion and dust production because of destruction of crust and vegetation (Nauman et al., 2018; Gillies et al., 2022; Goossens and Buck, 2009). Regional anthropogenic disturbances involve land use changes, agriculture, grazing, mining, construction, and military use (Duniway et al., 2019). While some of these processes may be deemed necessary or approved by larger governmental bodies, their negative impact on the local landscape is great.

One other type of anthropogenic disturbance is by off-highway vehicle (OHV) use, the popularity of which has increased dramatically in the past three decades. In Utah from 1998 to 2006 the number of registered OHVs tripled to over 170,000 vehicles (Smith et al., 2009). Utah's abundance of Bureau of Land Management (BLM) lands and ease of access to them has seen an increase in the number of recreators. This number was further increased during the COVID-19 pandemic and into 2021 (Utah, 2021). Destruction of vegetation, soil structure and natural soil properties like soil crusts have been observed at other OHV areas in the US and North America. (Goossens and Buck, 2009 Goossens et al., 2012 Hesp et al., 2009). Vegetation loss due to OHV activity is significant within Utah as observed by Nauman et al., (2018) with their findings showing OHV roads making up 7 to 8% of the regional dust emissions alone. Understanding the effects of anthropogenic soil disturbance can help inform future land management decisions that affect health and safety for both the soil and the recreators (Goossens and Buck, 2009).

In Utah, areas of playas and Lake Bonneville sediment have previously been identified, via MODIS satellite, as regional sources of dust emissions Hahnenberger and

Nicoll, (2014). Dust emissions from OHV sites are not as well documented in Utah compared to other anthropogenic dust sources, so we selected multiple popular OHV recreation areas including Bonneville Salt Flats, Knolls, Lone Rock, and Little Sahara composed of sand dunes, playas, and Lake Bonneville terrace sediments (Fig. 1). We aim to determine the dust emission potential of the selected OHV areas, as well as the impact of OHV activity on the landscapes and soil structure. Following ideas from Duniway et al., (2019) we hypothesize that: 1) disturbed surfaces will have an increased emission rate by an order of magnitude or more compared to undisturbed soils, and 2) the most emissive landforms are playas and lake terraces. To test these hypotheses, we used PI-SWERL (Portable In Situ Wind Erosion Laboratory) to measure particulate matter < 10 μm (PM 10) emissions as well as total suspended particulate (TSP) and compared dust emission potential with soil characteristics including grain size, soil crust strength, and soil structure.

Figure 1:Map of Utah and testing areas. OHV locations marked by red triangles.

Background: Dust Emission Processes

Dust emissions are facilitated by high winds above a threshold shear velocity, or the certain critical wind velocity required to cause initial disturbance of soil particles so that continuous movement occurs (Bagnold, 1941), low surface roughness (vegetation, rocks) and soil moisture. Surface roughness is important as it increases the shear velocity needed to entrain particles by slowing the wind. Surfaces with greater roughness then require greater shear velocity, and smoother surfaces, less shear velocity. Soil moisture plays a similar role as increased soil moisture lends greater cohesion between grains needing higher shear velocity to entrain grains off the surface. Dust emissions can be influenced by any of these above factors, and dust is generated through one of the following means: A) saltation bombardment, B) aggregate disintegration, C) aeolian abrasion, and D) aerodynamic entrainment (Fig. 2) (Sweeney, 2022).

Saltation bombardment is the process by which a mineral grain strikes and abrades a fine-grained substrate kinetically freeing dust. This processes' emissions vary based on the speed and height from which the grain strikes. Bombardment is limited by the supply of particles to saltate. Surfaces with high soil moisture or biocrust may not be very emissive (Belnap 2003).

Aggregate disintegration is where sand sized aggregates, composed primarily of silt and clay, break down during the processes of saltation and produces dust from the destruction of their form against a surface. Some aggregates are strong enough to abrade soil surfaces similarly to saltation bombardment. In surfaces like lake terraces with loamy textures, aggregate disintegration is a key process of dust emissions (Sweeney, 2022). Aeolian abrasion is the interaction between mineral grains directly chipping, spalling, or removing the coating on the grain surface which is directly influenced by the angularity of the grain and the speed at which grains collide. Softer and more brittle grains like gypsum are more easily abraded than minerals such as quartz, however even these harder grains can still produce significant amounts of dust (Whalley et al. 1982, 1987; Sweeney, 2022).

Aerodynamic entrainment is the direct emission of dust that is loose upon a surface without the presence of any other saltating grains or particles. This mechanism of dust entrainment is rare and requires weak inter-particle cohesion (Shao and Klose, 2016). This is only possible on surfaces with no vegetation, low soil moisture or on playas where the surface can be dried by the wind and thus decrease the threshold shear velocity required to entrain particles (Cornelis et al., 2004).

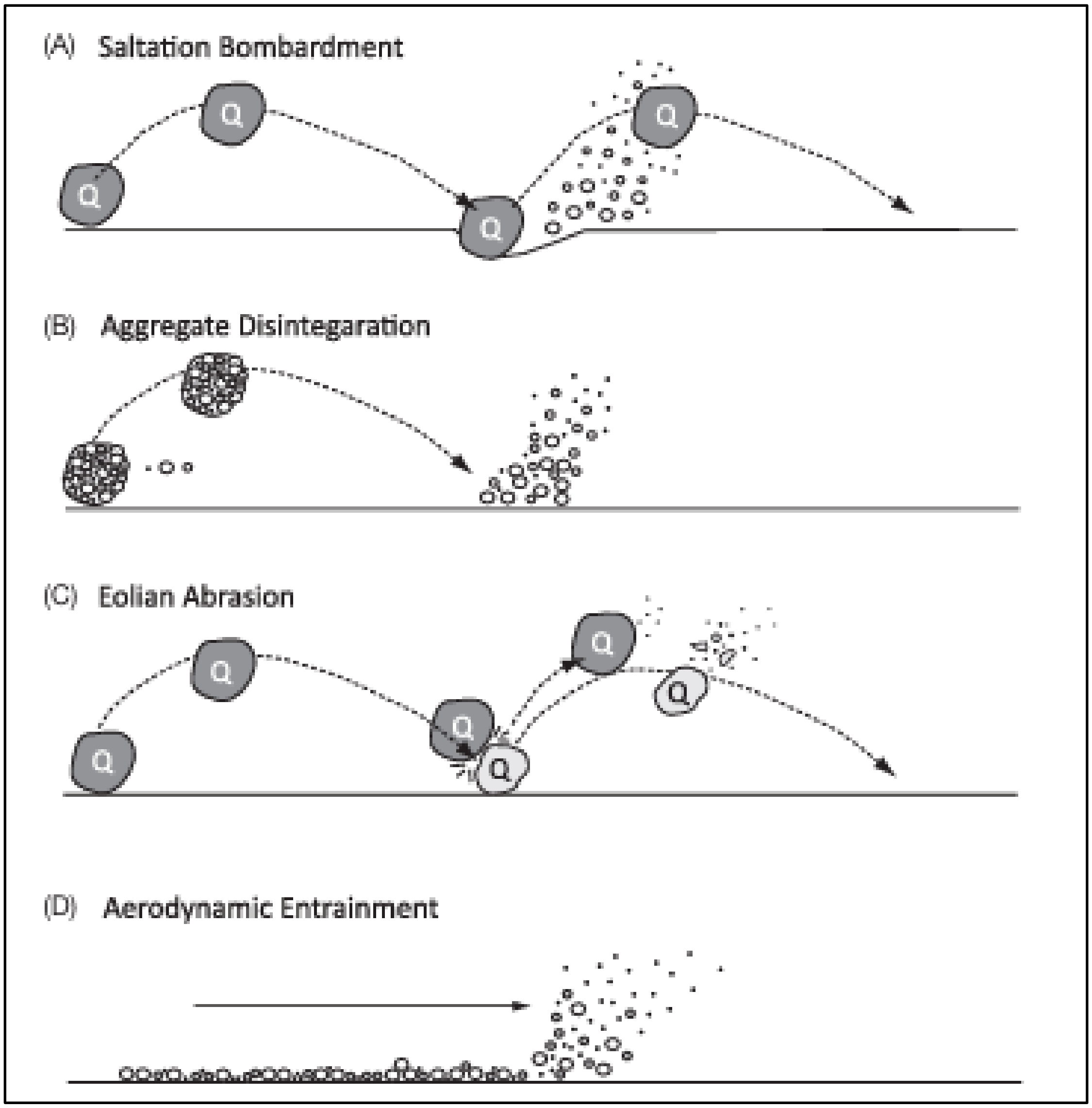

Figure 2): Dust emission process. Q =quartz grain. From (Sweeney, 2022)

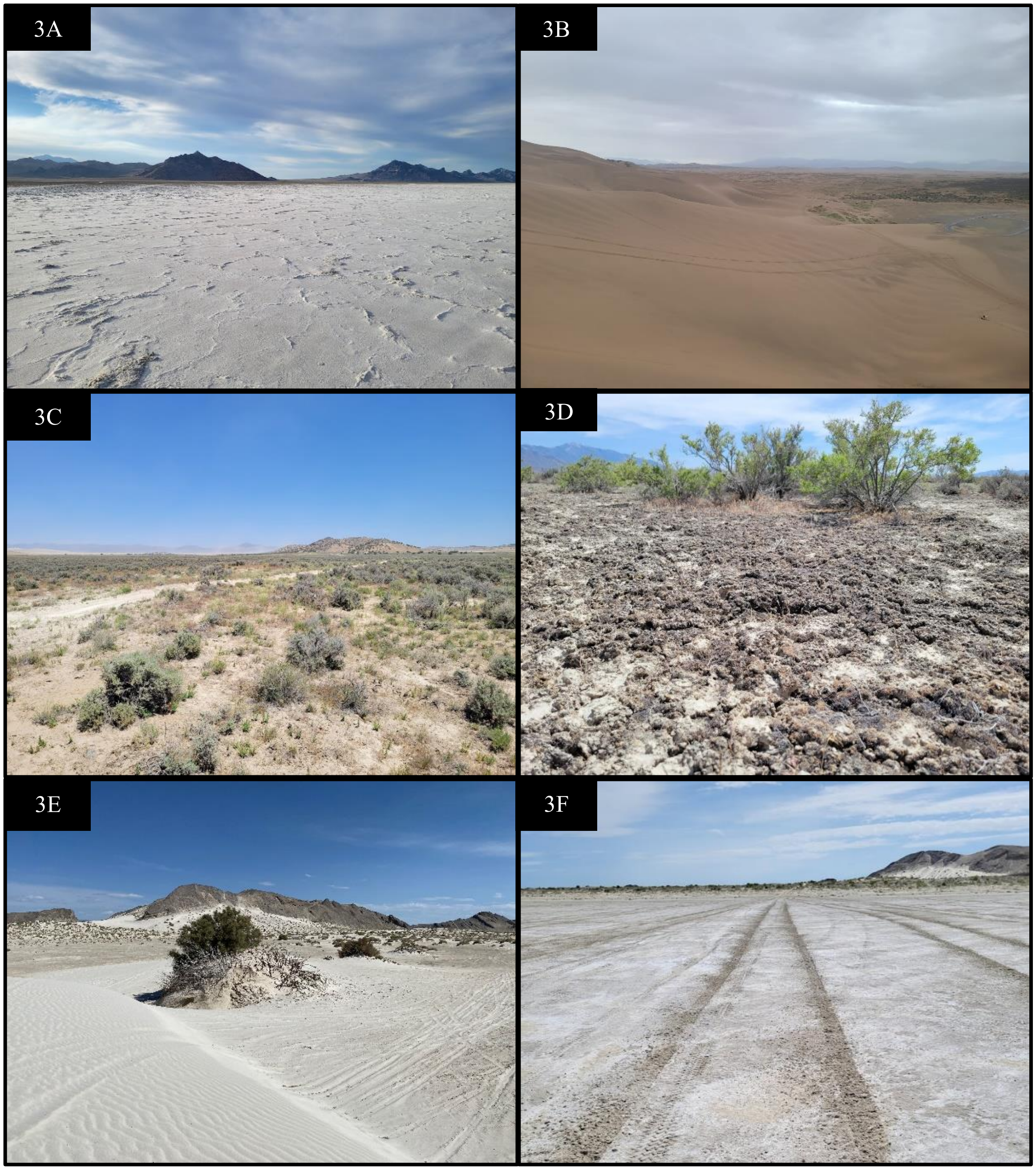

Figure 3: Photographs of various landforms across various OHV areas in Utah. 3A: Salt Flats at Bonneville Salt Flats. 3B: Sand Mountain at Little Sahara Recreation Area.3C: Undisturbed Lake Bonneville terrace at Lone Rock and a mix of physical and biological soil crusts. 3D: Biocrust on Lake Bonneville sediment at Lone Rock. 3E: Gypsum dunes at the Knolls OHV area. 3F: Disturbed playa at the Knolls OHV area.

Methods

Field work was conducted in 2022 and 2023 at various Bureau of Land Management areas in Utah: Lone Rock, Little Sahara, Bonneville Salt Flats, and the Knolls (Fig. 1, 2). In June of 2022, we conducted 81 PI-SWERL tests on both disturbed off-highway vehicle trails and adjacent undisturbed soils on landforms including lake terraces, dunes, and playas. In June of 2023 we added 25 field tests and replicated 3 sites to assess annual variability. A total of 114 PI-SWERL tests were conducted.

PI-SWERL or Portable *in situ* Wind Erosion Laboratory was used to measure dust emission potential at each of our sites. PI-SWERL is a 0.5 m diameter open bottom chamber with an annular blade 0.07 m above the testing surface; the testing diameter is 0.5 m (Fig. 4). The annular blade spins at pre-set RPM values to create shear velocity at the surface, calibrated to a smooth surface (Etyemezian et al., 2007). To correct the shear velocity for rough surfaces a surface roughness value, or alpha value, is applied based on a look-up table (Etyemezian et al., 2014; Hartshorn, 2023). We conducted two types of tests at each of our sites. The first test, a ramp test, increases constantly up to the set value of 5000 RPM and stops. The purpose of this is to identify the shear velocity at which entrainment of dust first occurs. The second test, a step test, increases in a stair step pattern by 1000 RPM intervals from 2000 to 5000 RPM. Each step is held for 60 s before increasing to the next RPM. The purpose of the step test is to calculate the dust flux from the shear velocities as they are increased from roughly 0.38 to 0.82 m/s.

Figure 4: Photograph of the PI-SWERL (right) with computer, battery and control box mounted on carriage (left).

Concentrations of dust in mg/m^3 were measured by two devices. Total suspended particulate was measured by a Casella Microdust PRO (Bacon et al., 2011; Sweeney et al., 2023) while PM10 (particulate matter <10 µm) was measured by a DustTrak II Model 8530 nephelometer (Etyemezian et al., 2007).

$$E_i = \frac{\sum_{begin,i}^{end,i}(C_i \times F \times t_o)}{\left(t_{end,i} - t_{begin,i}\right) \cdot A_{eff}}$$

Dust flux in mg/m^2 was calculated using the equation by Sweeney et al. (2011) where E_i is the flux of dust emitted at a given RPM, RPM is *i,* C is the concentration of dust, F is the rate that clean air enters the PI-SWERL's chamber, t_o is the frequency at which dust concentration data is being measured (1 s), A_{eff} is the area of the test chamber under the annular blade, and t_{end} and t_{begin} are the times at the beginning and end of each RPM step, which gives us the duration of the step.

Each test site consisted of paired disturbed and undisturbed landforms of the same type. These pairs were each tested with one ramp test and 2 or more step tests. We defined a disturbed landform based on these key characteristics: having tire tracks, cattle trails, or artificial disturbances on crusted trails with little to no vegetation, but these OHV trails can be crusted after rains. We defined an undisturbed landform based on the following key characteristics: crusted and/or vegetated surface, or otherwise natural surface with no evidence of disturbance.

At each testing site, the surface crust strength was measured using a Torvane which measures shear strength (Goossens, 2004), and penetrometer which measures normal strength (Li et al, 2004). Ten measurements using each device were taken at each site for both the disturbed and undisturbed landforms. Soil pits were dug at each site to observe soil horizons, structure, and color following Schoenenberger et al. (1998). Soil loss from disturbed sites was estimated by comparing the soil from undisturbed sites using soil pits. These measurements gave us the amount of soil missing from the vehicle trail compared to the level of the undisturbed soil. Soil samples were collected to determine presence of carbonates, bulk density, and grain size. Following determination of bulk density, subsamples were mixed in a 1:5 ratio of soil: deionized water suspensions to measure the electrical conductivity and salinity using a EC100 portable conductivity meter (Mason et al., 2011; Schoeneberger et al. 1998).

To determine grain size, we analyzed samples by dry sieve using a Gilson SS-3 performer III sieve shaker, and laser diffraction analysis using a Malvern Mastersizer 2000. The Malvern determines the volume of particles that are sand, silt, and clay. While clay is considered <4 µm, the Malvern underestimates clay at this size and so the cutoff is 7 µm (Konert and Vandenberghe, 1997). Samples were analyzed with the Malvern two ways: with pretreatment and without. Pretreated samples were mixed with a dispersant, sodium hexametaphosphate, to break apart aggregates. Samples with a high aggregate population disintegrate following pretreatment leading to an increase in the amount of finer material (Mason et al., 2011). Both the sieve analysis and Malvern without pretreatment allowed the determination of sand-sized aggregates within the soil samples, as compared to soil textures typically determined following aggregate destruction.

A 2008 Rigaku Ultima IV x-ray diffractometer (XRD) unit, using copper K-alpha radiation, was used for these analyses. A 2021 Rigaku software package (SLSII) was used for data background correction and peak identification. Observed peak positions were search-matched against the International Centre for Diffraction Data (ICDD) Joint Committee on Powder Diffraction System (JCPDS) card database (PDF2; release 2021) for mineralogical results.

XRD sample sizes were obtained using the quartering method, until a sample weight of approximately 4 to 5 grams was collected. The samples were then ground by hand using a mortar and pestle and sieved until all particles passed through a 100-mesh

(150 micron) screen. After sieving, the dry powdered samples were blended with a spatula to help reestablish a uniform distribution of the minerals throughout the powder. A representative portion of each sieved sample was placed in a small sample holder for XRD analysis. X-ray diffraction analysis was conducted following procedures outlined in Schoenenberger et al. (2012).

Results

Each ORV site had a variety of landforms except Bonneville Salt Flats, composed primarily of salt playa. The Knolls had all three landforms: lake terraces, gypsum dunes, and playas. Lone Rock was composed of lake terraces and playas. Little Sahara was composed of quartz dunes and lake terraces (Table 1) (Fig 3.). The source of these lake terraces is linked back to Pleistocene Lake Bonneville. Playas are seasonally wet landforms, primarily flat and dominated by salt and finer grained sediments. Finally, dunes are composed of quartz or gypsum depending on ORV area.

PI-SWERL dust emission potential is compared at a shear velocity of 0.6 m/s which corresponds to a 10 m windspeed of approximately 20 to 33 m/s for both PM10 and TSP dust (Merrill, 2023). PI-SWERL sites were grouped by landform in disturbed (off road vehicle track) and undisturbed (soil adjacent to track) conditions. For PM10, dunes generally showed little difference in emissivity when disturbed or undisturbed because of the bare, well-sorted nature of the dune sand emitting on average 1.0 $mg/m^2/s$. An exception is for site K16, a lunette dune that emitted 14.4 $mg/m^2/s$ when disturbed, the highest flux among landforms (Fig. 5A), compared to the very low flux of the undisturbed vegetated surface (0.01 $mg/m^2/s$). Lake terraces emitted 0.02 $mg/m^2/s$ on average, with lower emissions on surfaces with vegetation or biological soil crust, compared to maximum emissions of 13.0 $mg/m^2/s$ on disturbed surfaces. Playas emitted the least amount of dust with 0.005 $mg/m^2/s$ on average and a maximum of 3.3 $mg/m^2/s$ when disturbed. Disturbed surfaces emitted one to five orders of magnitude more dust than their undisturbed counterparts (Fig 5).

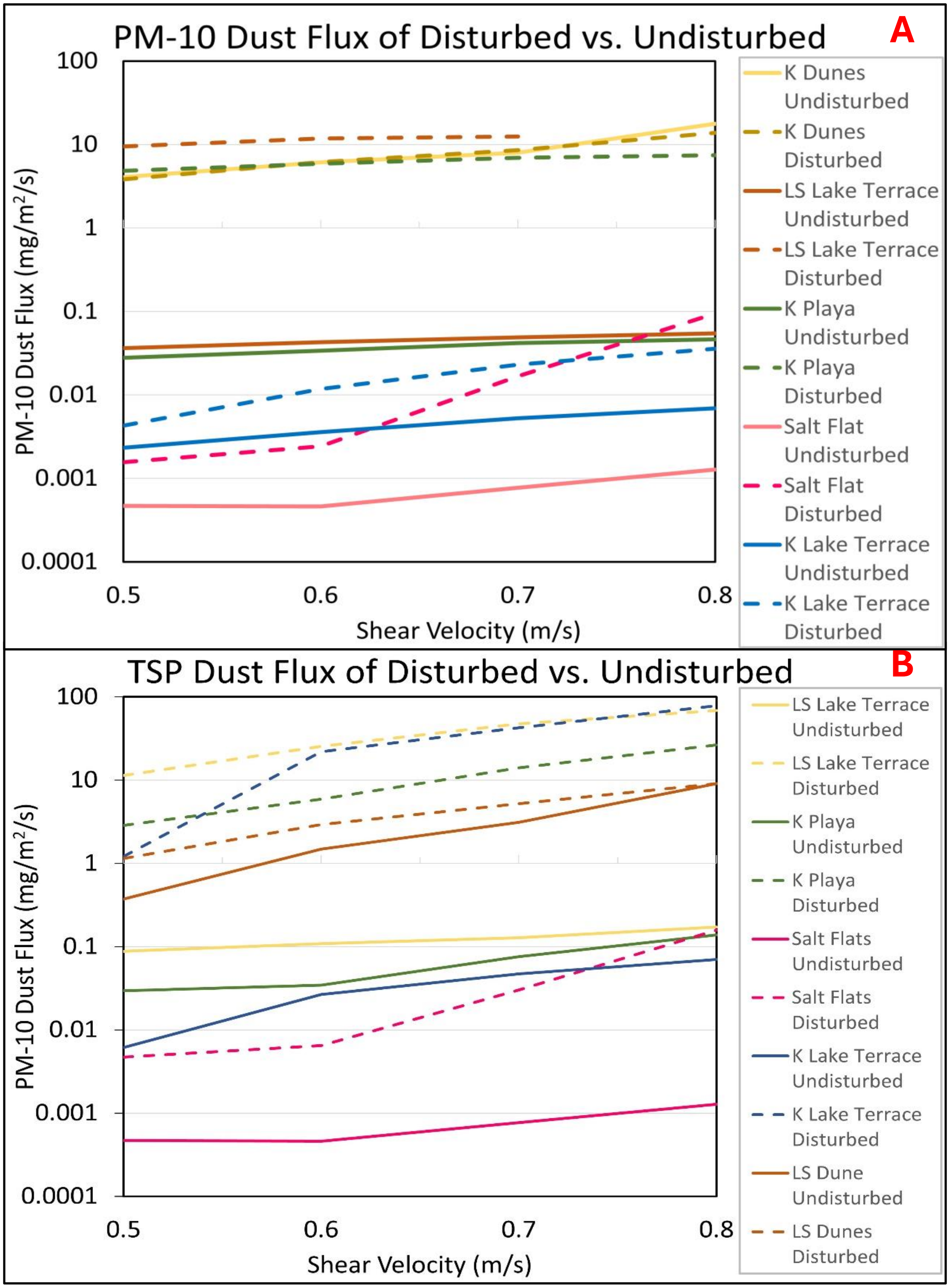

Figure 5: A & B:PM-10 flux disturbed and undisturbed landforms sites depicted are typical or representative of landforms at their respective OHV areas. Dashed lines represented disturbed landforms and are color matched to their solid undisturbed counterpart. B same as in A but TSP data.

TSP measurements typically emitted twice that of PM10 also at 0.6 m/s (Fig. 5B). Disturbed dunes had a higher on average emission, 3.1 $mg/m^2/s$ compared to 1.0 $mg/m^2/s$ for undisturbed. K16 again stands out as the highest emitter of dunes at 18.2 $mg/m^2/s$. Lake terraces on average emitted 0.07 $mg/m^2/s$, with great variability between disturbed, LS2 emitting 132.4 $mg/m^2/s$, and undisturbed effectively emitting 0.0 $mg/m^2/s$ on LR1's vegetated surface. Playas continued to emit the least with an average of 0.005 $mg/m^2/s$ and a max of 5.9 $mg/m^2/s$ on disturbed surfaces. The maximum flux on undisturbed surfaces was at K7 with 0.04 $mg/m^2/s$ (Table 1).

Table 1: Shows landform percentage of each OHV area, the maximum PM-10 flux of each landform and% sand for each landform at each recreation area.

Recreation Area and Landform	Area %	Max Flux Undisturbed $mg/m^2/s$	Max Flux Disturbed $mg/m^2/s$	% Sand Dispersed	% Sand Not Dispersed
Knolls					
--Dune	21	15.92	53.60	93.72	99.15
--Playa	46	.54	26.49	40.21	49.14
--Lake Terrace	30	.74	78.47	47.06	67.03
Little Sahara					
--Dune	35	9.36	9.09	93.33	99.46
--Playa	ND*	ND	ND	ND	ND
--Lake Terrace	45	.21	229.83	54.20	69.72
Lone Rock					
--Dune	ND	ND	ND	ND	ND
--Playa	24	.02	0^	19.21	24.39
--Lake Terrace	24	0^	234.12	30.01	40.54
Bonneville Salt Flats					
--Playa	97	0^	.16	ND	81.14

* ND = no data, 0^ = near zero.

Crust strength

The shear strength of crusts as measured by Torvane at undisturbed sites was higher on average compared to disturbed sites (Fig. 6) (Table 2). Lake terraces and playas both had undisturbed median shear crust strengths of about 1 kg/cm^2. Crust strengths for disturbed lake terrace and playa sites were one order of magnitude lower than undisturbed sites (0.20-0.36 kg/cm^2). Dunes had similar crust strength for undisturbed (0.19 kg/cm^2) and disturbed (0.12 kg/cm^2).

Penetrometer measurements for all undisturbed sites were higher on average than Torvane measurements except for playas (Fig. 7) (Table 2). Disturbed playas had the highest average compressive crust strength of about 4 kg/cm^2. The undisturbed playas average strength was roughly 0.60 kg/cm^2. For lake terraces both undisturbed and disturbed surfaces had averages ranging from 0.70-0.40 kg/cm^2 respectively. Undisturbed dunes had the greatest range of crust strength having both the lowest of >0.008 kg/cm^2 but a higher average than that of its disturbed average of 0.1 kg/cm^2.

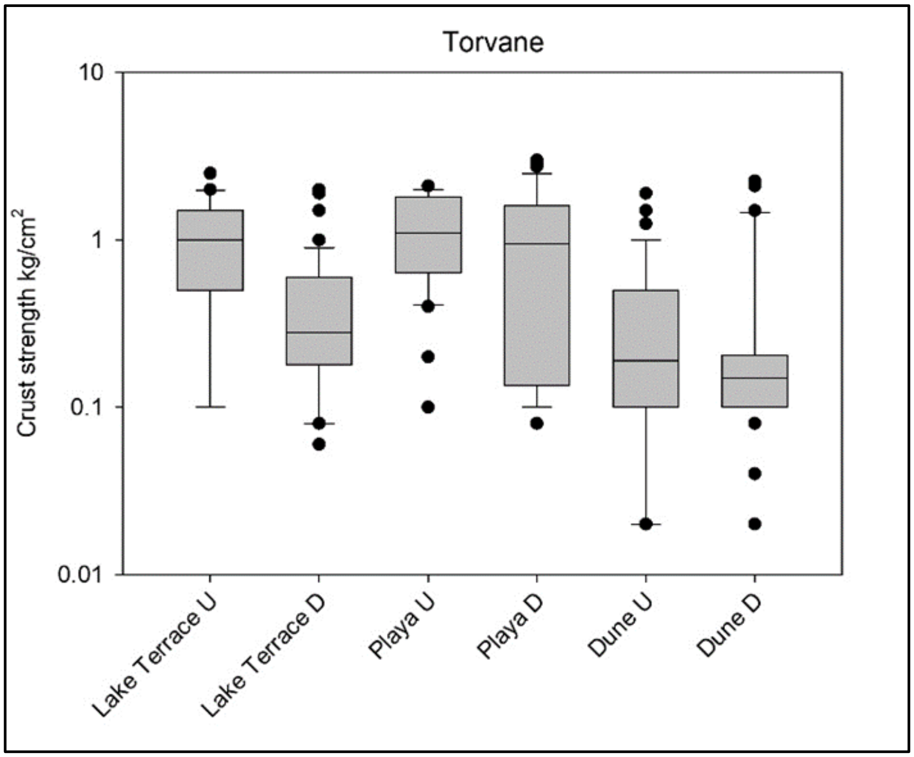

Figure 6: Torvane shear crust strength by landform, disturbed (D) and undisturbed (U) measured in kg/cm^2.

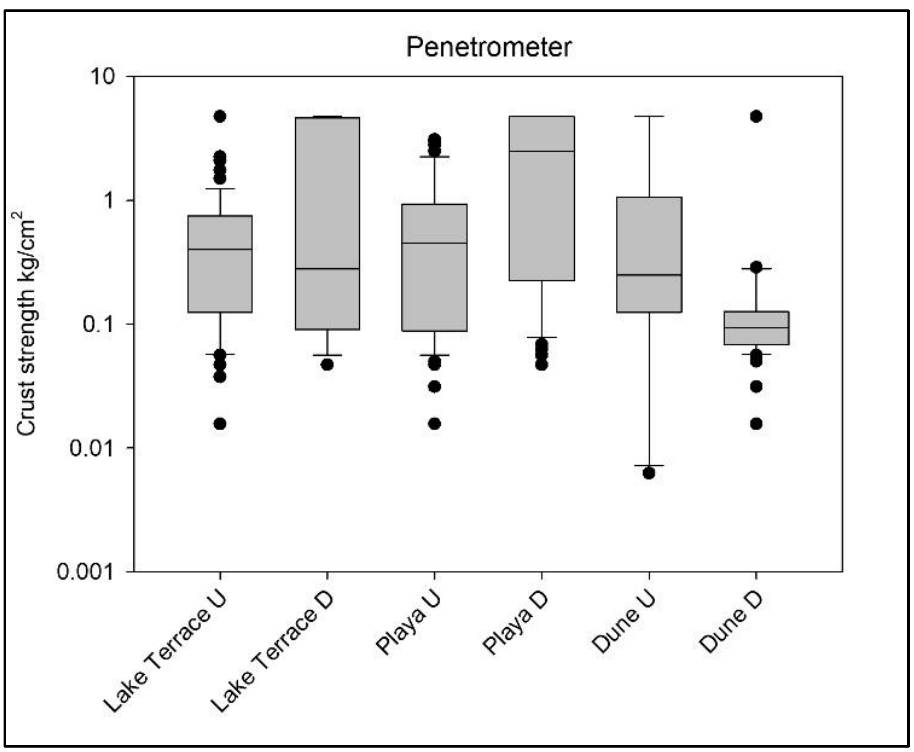

Figure 7: Penetrometer crust strength by landform, disturbed (D) and undisturbed (U) measured in kg/cm^2.

Table 2: List of sites with bulk density, Electrical Conductivity (EC), Torvane, and Penetrometer values as well as the disturbance of the landform.

Landform	Site	Soil Series	Disturbance	Bulk density g/cm^3	Torvane kg/cm^2	Penetrometer kg/cm^2	EC Descriptors	EC (dS/m)
Lake	LR1	Skrumpah	U	ND	0.51	0.38	Nonsaline	0.42
Lake	LR2	Skrumpah	D	1.38	0.525	2.06	Nonsaline	0.55
Playa	LR3	Playa	U	1.39	1.82	0.66	Slightly Saline	6.61
Playa	LR4	Playa	D	1.46	2.22	1.60	Slightly Saline	7.36
Lake	LR5	Skrumpah	U	1.42	1.225	1.15	Nonsaline	0.85
Dune	K1	Dynal	U	ND	0	4.75	Nonsaline	0.29
Dune	K4	Dynal	D	ND	0	0.18	Nonsaline	0.30
Lake	K6R-1*	Tooele	D	1.46	0.66	0.10	Slighlty Saline	4.49
Lake	K6R-4	Tooele	U	1.24	0.96	0.07	Very Slightly Saline	3.83
Playa	K7R-1	Playa	U	1.45	1.35	0.16	Slightly Saline	3.13
Playa	K8	Playa	D	ND	1.33	3.85	Slightly Saline	2.20
Playa	K9	Playa	U	ND	0.6	0.10	Nonsaline	0.91
Playa	K10	Playa	D	ND	0.126	0.08	Nonsaline	1.59
Lake	K11R-1	Tooele	U	1.13	1.175	0.07	Nonsaline	0.38
Lake	K12	Tooele	D	ND	0.242	0.09	Nonsaline	0.52
Dune	K13	Dynal	U	1.26	0.27	0.24	Nonsaline	0.30
Dune	K14	Dynal	D	1.26	0.118	0.07	Nonsaline	0.28
Lake	K15-1	Izamatch	U	1.42	1.275	0.67	Nonsaline	0.28
Lake	K15-4	Izamatch	D	1.41	0.805	2.00	Nonsaline	0.28
Dune	K16-1	Dynal	D	1.18	0.141	1.05	Nonsaline	0.22
Dune	K16-4	Dynal	U	1.40	0.695	0.01	Nonsaline	1.38
Lake	LS1	Woodrow	U	1.14	0.3	0.55	Nonsaline	0.33
Lake	LS2	Woodrow	D	1.53	0.19	0.17	Nonsaline	0.24
Lake	LS3	Goldrun	U	1.24	1.45	1.06	Nonsaline	0.28
Lake	LS4	Goldrun	D	1.35	0.258	0.32	Nonsaline	0.25
Dune	LS5	Duneland	U	1.60	0.133	0.15	Nonsaline	0.08
Dune	LS9	Duneland	D	1.54	1.465	0.08	Nonsaline	0.09
Playa	BSF1	Salt Flats	D	ND	0.144	0.07	Strongly Saline	18.86
Playa	BSF2	Salt Flats	U	ND	ND	4.75	Strongly Saline	18.86

U= Undisturbed, D = Disturbed

Soil descriptions

In the upper 30 cm of soil, typical soil structure of undisturbed soils included fine to medium sub angular blocky for dunes, platy, sub angular blocky to coarse granular for lake terraces, and fine to medium platy structure for playas. Disturbed playas had the same structure of fine to medium platy, disturbed lake terraces were typically fine angular blocky to sub angular blocky. Dunes were similar for disturbed and undisturbed. For lake terraces with well-established trails the soil structure in the upper part of the soil was destroyed as indicated by a loose, powdery consistency underlain by hard, compact soil. Lake terraces had the greatest loss of A horizon depth, with disturbed surfaces containing 0 or only 6 cm of the original A horizon compared to adjacent undisturbed soil. Some areas saw dramatic loss of A horizon and modification forming deep rutted trails (Fig. 8). Disturbed lake terraces sites did retain some of their original A horizon material, however, this was often made up of pulverized A horizon and surface material which is easily entrained by the wind. Based on the soil profiles in the paired undisturbed and disturbed soil pits, we estimated soil erosion from the undisturbed sites ranging from 5 to 40 cm. Dunes had no soil development if they were active and soil erosion could not be determined. For vegetated dunes containing physical and or biological crust on the surface, we documented up to 30 cm of erosion on trackways. Playas do not contain developed soils, so erosion or compaction was determined by depth of vehicle tracks. Disturbed playa had much greater compaction due to ruts, with strong platy structure and few to no pores compared to weak platy structure and many pores in undisturbed playa.

Figure 8: Disturbed trail with substantial amounts of soil loss.

Bulk density

Disturbed landforms generally had higher bulk density for both lake terraces and playas. Disturbed lake terraces landforms had a larger 0.17 g/cm^3 difference between its disturbed and undisturbed averages (Table 2). Undisturbed landforms had consistently lower bulk density, however playas were often difficult to sample due to the compaction and hard surface, which made collecting bulk density samples impossible in some cases.

Electrical Conductivity

Playas were much more saline compared to other landforms with a range of 0.91 to 18.86 dS/m and an average of 7.44 dS/m. BSF had the highest values over 18, making them strongly saline. For dunes and lake terraces the salinity class ranged from non-saline to slightly saline with a range from 0.08 to 4.49 dS/m (Table 2).

Grain size

Dune sands were not pretreated prior to analysis in the Malvern because some sands are composed of gypsum and are soluble. Most samples contained >90% sand and the soil texture is classified as sand (Fig. 9). Playa samples that were dispersed prior to analysis ranged from clay loams to sandy loams, containing 9-59% sand. Non-dispersed samples were coarser, with textures from silt loam to sandy loam and sand contents from 15-71%. The Malvern could not analyze Samples from Bonneville Salt Flats because they are composed primarily of halite and are soluble in water. These samples were still sieved manually without water using standard sieves to compare sand and silt percentages. Lake terrace samples that were dispersed had soil textures ranging from clay loam to sand, with sand contents of 16-91%. Non-dispersed lake terrace textures were coarser, containing 33-85% sand. Disintegration of sand size aggregates likely contributed to this trend of decrease size percentages within the Malvern samples. Undisturbed samples for playas and dunes tended to be coarser grained than undisturbed soils (Figs. 8 and 9).

Mineralogy

Mineralogy of lake terraces primarily contained quartz with minor amounts of bassanite, calcite, or plagioclase. Dunes tended to be dominated by gypsum (Knolls) or quartz (Little Sahara), while also having minor calcite or aragonite. Bonneville Salt Flats had the most unique mineral make up composed mostly of halite with some gypsum, anhydrite, bassanite and sylvite.

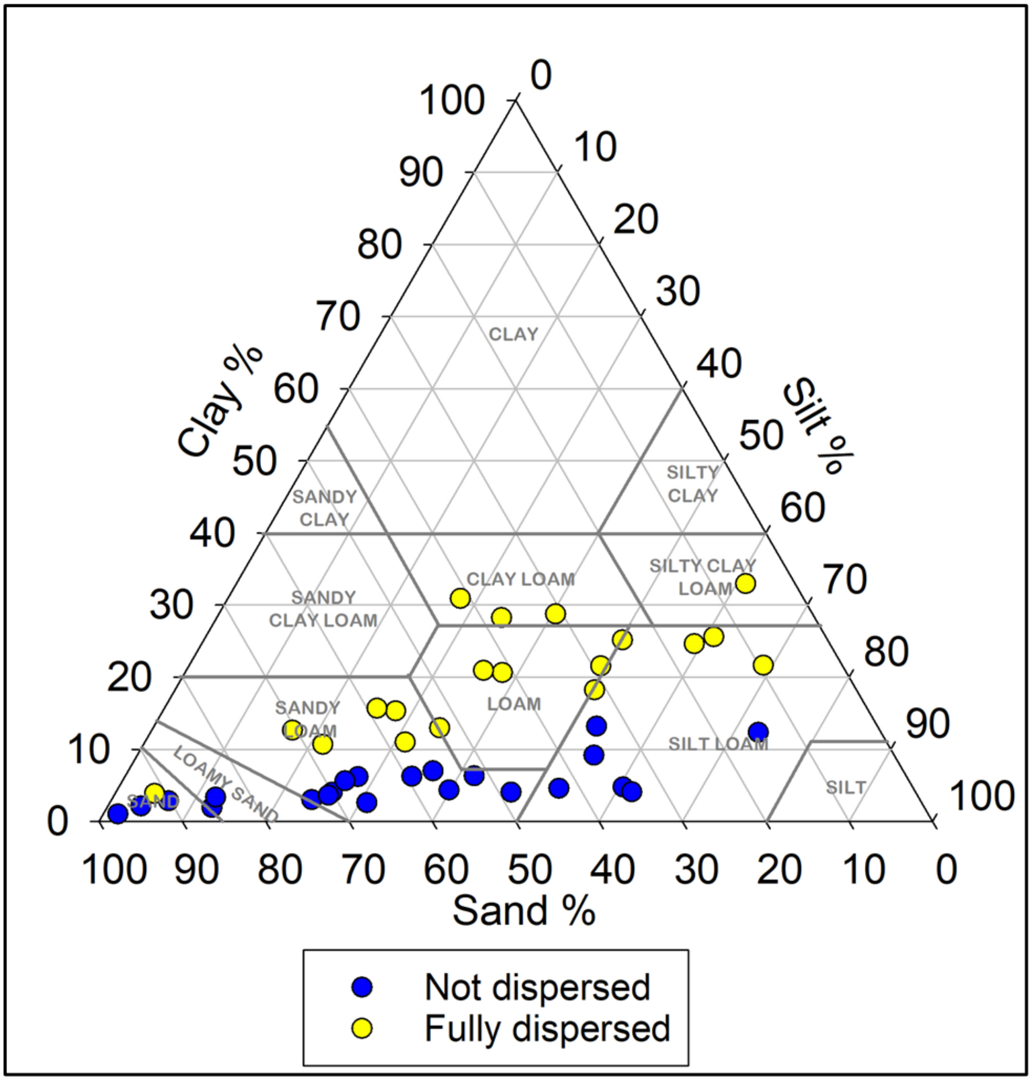

Figure 9: texture triangle representing dispersed and non-dispersed samples from Malvern pretreated and non-pretreated samples.

Discussion

The dust emission potential for our sites verified previous work by Hahnenberger and Nicoll (2012) that cites anthropogenic activities as contributing to and corresponding with dust storms in Utah. Lake Bonneville terrace sediments were the highest emitters of dust when protective crusts and vegetation were removed (Fig. 5). Disturbed lake terrace fluxes are up to 5 orders of magnitude greater for both PM-10 and TSP (Fig. 5) than undisturbed surfaces. Lake terraces are more emissive due to a combination of grain size, lack of soil crusting, and vegetation compared to the undisturbed counterpart, which has physical crusts, biological crusts, and vegetation cover. Soils with well-developed physical crusts or high soil moisture such as in playas also result in low emissions such as LR3 the low emitter for playas at Lone Rock (Table 1). Landforms like playas with high clay percentage emitted less than sites with higher sand and silt percentage. Gypsum dunes at the Knolls are the most emissive undisturbed landform because of their lack of crusts and aeolian abrasion between gypsum grains (Fig. 5). Lake terraces are the lowest emitters when stabilized with vegetation and biological soil crusts (Fig. 5). Disturbed surfaces always produced a higher level, one to five orders of magnitude of dust emissions. Making the driving surface more susceptible to wind erosion, similar to findings by Goossens and Buck (2009). Results from Goossens and Buck (2009), found that disturbed surfaces with higher silt content such as lake terraces were one to five times as emissive than undisturbed soils which corresponds with our results for maximum and minimum fluxes (Table 1).

Grain size for disturbed surfaces showed an increased finer grain population likely due to physical disturbance in lake terraces by OHVs based on data from the

Malvern and the texture shifts (Fig. 9) from both disturbed and undisturbed samples (see appendix A). These fine grains are already present in the soil or trapped in aggregates which can be broken down by the disturbance of OHVs. Aggregates are indicated in the sieve and non-dispersed grain size data, which contain higher percentages of sand compared to the dispersed grain size data where aggregates were destroyed in pretreatment prior to analysis (Fig. 10). Similarly, playa samples also have a shift towards finer grains in the Malvern data likely due to the dissolving of salt in the aqueous solution as well as breakdown of aggregates. Some samples such as LR2 show a sand percentage decrease of almost 50% shifting from sand sized particles to silt and clay in the dispersed samples (Appendix A). Dunes composed primarily of mineral sand do not contain aggregates and so do not display a big shift in grain size between disturbed and undisturbed soils (Fig. 10). Many of the dunes at the Knolls are dominantly gypsum which is more easily abraded via aeolian processes (Sweeney et al., 2023). Quartz dunes are also emissive when disturbed as found in PI-SWERL data from Gillies et al. (2022) who documented that average disturbed fluxes at shear velocity of 0.6 m/s were 1.7 to 2.5 times as emissive compared to non-disturbed dunes. This emissivity was very consistent with our findings at Little Sahara's quartz rich dunes at a shear velocity of 0.6 m/s (Appendix B). The heterogeneous mixing of grain sizes at sites such as LR2, LS3, and LS4, lake terraces with high sand% (Appendix A) increases the production of dust via saltation bombardment of larger grains onto a crusted surface or grain to grain collisions (Sweeney, 2022).

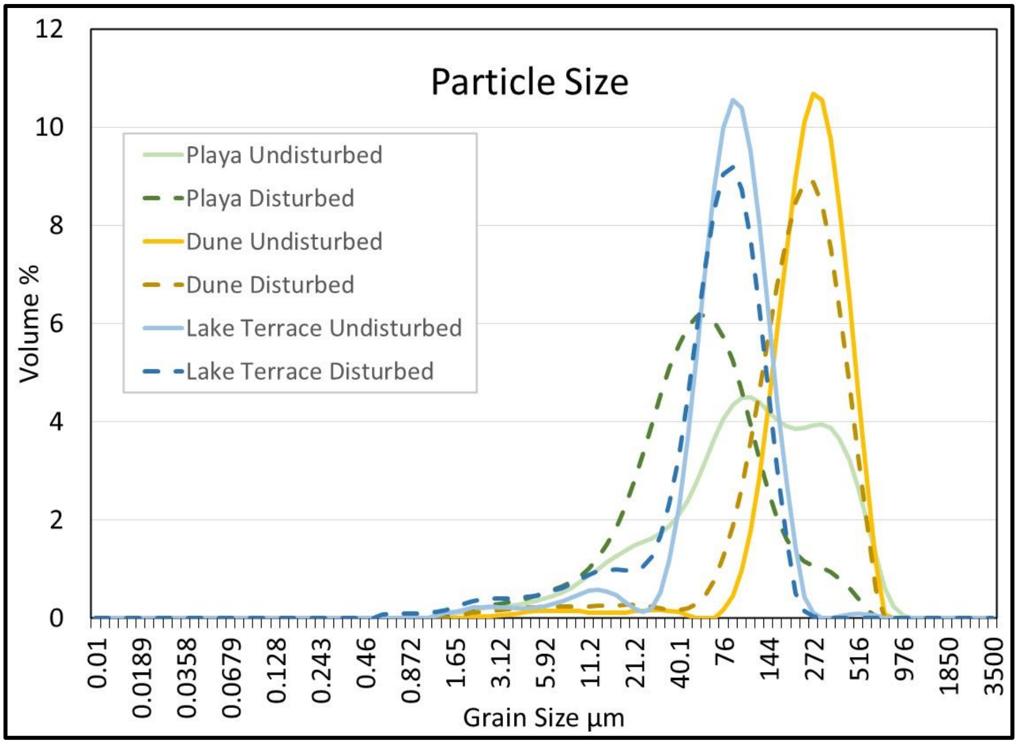

Figure 10: Grain size comparison between samples that were disturbed and not disturbed. The disturbed samples had an increased population of finer grains likely due to the breakdown of sand sized aggregates due to anthropogenic disturbance.

Repeated vehicle use over areas pulverizes the upper surfaces of the soil and compacts the subsurface. We observed noticeable differences in emissivity and silt sized particles on surfaces with and without crusting. Physical and biological crusting (Fig. 3D) has a positive role in mitigating emissions similar to findings by Rodriguez-Caballero et al. (2022) (Table 1). These crusts are susceptible to anthropogenic disturbance and when destroyed leave behind hard compacted surfaces or continue to erode away into deeper trails. The crust strength for both disturbed lake terraces and disturbed playas have higher strength at the 7th percentile. (Fig. 6, 7). This could be due to the soil compaction, increasing the compressive strength of these soils. Torvane measurements found disturbed strength is less than undisturbed, indicating that disturbance is destroying soil structure (Fig. 6). Notably the Bonneville salt flats undisturbed sites were too hard to measure, maxing out the Torvane and Penetrometer. However, in the case of Bonneville and other salt dominated crusted playas, the crust reformed on disturbed surfaces almost immediately, due to the salt. Losing higher crusts strengths indicates that the loss of the crusts creates soils that are unlikely to support vegetation or sequester dust via crusting. Soil pits dug at these locations support this by having few pores with higher bulk density due to compaction at disturbed sites compared to undisturbed (Table 2). Many of the playas at Lone Rock and the Knolls playas also had high bulk density (>1.40 g/cm^3) or were too hard to collect bulk density samples properly. Emissivity of playas may have been limited due to the higher soil moisture in addition to consistent crusting on playa surfaces. Studies by Merrill (2023) indicate that on playa landforms or landforms lacking vegetation having approximately 4% gravimetric soil moisture is enough to suppress dust emissions. Soil moisture was particularly high on the playas at Lone Rock, up to 18%. Similarly, the values for playas were higher in moisture and EC levels (Table 2) indicating higher salinity and greater cohesion and resistance to aeolian abrasion or saltation bombardment (Bowen et al. 2018; Merrill 2023).

OHVs function as an artificial accelerator of the natural aeolian processes to break down grains and create surfaces more likely to emit dust by pulverizing the upper crusts and horizons of landforms. This accelerated destruction of landforms negatively contributes to many issues for human health due to inhalation of dust particulates (Hahnenberger and Nicoll, 2012; Maddox, 2012). Directly destroying vegetation and biological crusts reduces the stability of the soils and decreases the wind speed necessary to entrain dust particles (Hesp et al., 2009). This increase in dust also impacts local and statewide visibility by increasing the likelihood of dust storm events (Ashley et al., 2015).

Anthropogenic alteration is also compounded by increased effects of climate change as droughts and continued increases in people participating in OHV activities make more trail development likely.

Conclusions

Breaking new trails off from established trails creates positive feedback as erosion by OHV use promotes further erosion for soils as it weakens the defensive properties of the crusts and vegetation while creating an avenue for erosion to occur. This anthropogenic feedback is subject to natural factors as well with prolonged droughts observed in Utah (Khatri and Strong, 2020) contributing negatively to the growth of vegetation and drying out and eroding soils during regional wind events. OHV activities present a unique and growing concern to both recreators and the landscape, as improper treatment of the landscape negatively impacts the health of people due to the inhalation of dust, but also the vegetation and soils that support the local environment. Our results show that disturbed surfaces emit at least one order of magnitude more than undisturbed surfaces, in support of what we hypothesize that: 1) disturbed surfaces will have an increased emission rate by an order of magnitude or more compared to undisturbed soils, and 2) the most emissive landforms are playas and lake terraces. Lake terraces were correctly identified as the landform with the most potential to emit high levels of PM-10 dust particles, but also the highest amount of total suspended particulate, in support of hypothesis 2, but playas had low emission potential, likely due to soil moisture and crusting.

While the total risk of dust emissions is dependent on many contributions of each process of dust emissions, our recommendations is for the future of recreational trail development among Utah's many OHV areas is to limit trails, as best possible, to landforms such as dunes and playas. Moving OHV driving to surfaces such as dunes is recommended based on other studies and results that similarly found moving away from naturally dust trapping or dust rich areas with high silt or natural biocrusts to be the best recommendation (McLaurin et al., 2011). Dunes stand out as the best candidate for trails as they have little variation in dust emissions whether disturbed or undisturbed. Playas similarly require repeat vehicle disturbance to reach higher emissions. All landforms are further protected by the presence of high moisture within the soil structure and the state of the soil crusting, both physical and biological, across all landforms. Responsible and informed management and recreator participation at these OHV areas is key to limiting our current impact on these landforms for our future use, but also the preservation of these natural areas. Emphasizing the protection of dust mitigating properties of soils should be a high priority among users of these recreation areas for the health of the landscape and the people.

Appendices:

Appendix A: grain size table by site. U= Undisturbed, D= Disturbed

Landform	Site	Soil Series	Disturbance	Soil Texture	%Clay	%Silt	%Sand	Soil Texture2	%Clay3	%Silt4	%Sand5	Bulk density g/cm3	Torvane kg/cm2	Penetrometer	EC (µS/cm)	EC (dS/m)
Lake	LR1	Skrumpah	U	Silt Loam	24.61	59.12	16.27	Silt Loam	9.16	54.82	36.03	ND	0.51	0.38	421	0.42
Lake	LR2	Skrumpah	D	Silt Loam	24.6	59.1	16.27	Silt Loam	13.2	53.1	33.7	1.38	0.525	2.06	553	0.55
Playa	LR3	Playa	U	Silt Loam	21.6	68.9	9.44	Silt Loam	12.3	72.9	14.8	1.39	1.82	0.66	6610	6.61
Playa	LR4	Playa	D	Loam	21.5	49.5	28.97	Sandy Loam	4.1	44	51.9	1.46	2.22	1.60	7360	7.36
Lake	LR5	Skrumpah	U	Silty Clay Loam	33.0	61.1	5.94	Sandy Loam	6.3	41.8	51.9	1.42	1.225	1.15	851	0.85
Dune	K1	Dynal	U	ND	ND	ND	ND	Sand	2.84	6.94	90.22	ND	0	4.75	286	0.29
Dune	K4	Dynal	D	ND	ND	ND	ND	Sandy Loam	5.61	26.7	67.67	ND	0	0.18	302	0.30
Lake	K6R-1*	Tooele	D	Loam	20.61	38.1	41.3	Sandy Loam	3	24.03	73	1.46	0.66	0.10	4490	4.49
Lake	K6R-4	Tooele	U	Clay Loam	28.24	34.2	37.56	Sandy Loam	6.22	34.43	59.34	1.24	0.96	0.07	3830	3.83
Playa	K7R-1	Playa	U	Sandy Loam	15.68	25.52	58.79	Silt Loam	4.74	60.52	34.74	1.45	1.35	0.16	3130	3.13
Playa	K8	Playa	D	Clay Loam	28.74	40.43	30.83	Sandy Loam	4.02	47.44	48.55	ND	1.33	3.85	2200	2.20
Playa	K9	Playa	U	Silt Loam	25.58	60.99	13.43	Sandy Loam	3.58	25.72	70.72	ND	0.6	0.10	914	0.91
Playa	K10	Playa	D	Sandy Loam	10.98	31.25	57.79	Silt Loam	4.57	52.9	42.54	ND	0.126	0.08	1585	1.59
Lake	K11R-1	Tooele	U	Sandy Loam	15.3	27.95	56.76	Sandy Loam	6.18	27.98	65.79	1.13	1.175	0.07	384	0.38
Lake	K12	Tooele	D	Sandy Loam	12.94	34.43	52.63	Sandy Loam	4.03	25.98	69.97	ND	0.242	0.09	519	0.52
Dune	K13	Dynal	U	ND	ND	ND	ND	Sand	1.01	1.76	97.23	1.26	0.27	0.24	302	0.30
Dune	K14	Dynal	D	ND	ND	ND	ND	Sand	2.12	3.98	93.89	1.26	0.118	0.07	284	0.28
Lake	K15-1	Izamatch	U	ND	ND	ND	ND	ND	ND	ND	ND	1.42	1.275	0.67	275	0.28
Lake	K15-4	Izamatch	D	ND	ND	ND	ND	ND	ND	ND	ND	1.41	0.805	2.00	276	0.28
Dune	K16-1	Dynal	D	ND	ND	ND	ND	ND	ND	ND	ND	1.18	0.141	1.05	224	0.22
Dune	K16-4	Dynal	U	ND	ND	ND	ND	ND	ND	ND	ND	1.40	0.695	0.01	1375	1.38
Lake	LS1R	Woodrow	U	Sandy Loam	12.63	16.9	70.46	Loamy Sand	1.9	12.61	85.49	1.14	0.3	0.55	331	0.33
Lake	LS2R	Woodrow	D	Loam	20.92	35.7	43.36	Loamy Sand	3.33	12.33	84.33	1.53	0.19	0.17	240	0.24
Lake	LS3R	Goldrun	U	Silt Loam	25.14	50.25	24.61	Sandy Loam	6.98	36.61	56.39	1.24	1.45	1.06	278	0.28
Lake	LS4R	Goldrun	D	Sand	3.84	4.75	91.41	Sandy Loam	4.32	39.86	55.83	1.35	0.258	0.32	246	0.25
Dune	LS5	Duneland	U	Silt Loam	18.22	50.36	31.41	ND	ND	ND	ND	1.60	0.133	0.15	81.3	0.08
Dune	LS9	Duneland	D	ND	ND	ND	ND	ND	ND	ND	ND	1.54	1.465	0.08	87.5	0.09
Playa	BSF1	Salt Flats	D	ND	ND	ND	ND	ND	ND	ND	ND	ND	0.144	0.07	18860	18.86
Playa	BSF2	Salt Flats	U	ND	ND	ND	ND	ND	ND	ND	ND	ND	ND	4.75	18860	18.86

Appendix B: Dust flux with alpha corrections by landform

Dunes					Lake Terraces					Playas				
Site	**0.5**	**0.6**	**0.7**	**0.8**	Site	**0.5**	**0.6**	**0.7**	**0.8**	Site	**0.5**	**0.6**	**0.7**	**0.8**
K1-2	1.115	3.118	5.915	9.386	LR1-2	0.001	0.001	0.002	0.002	LR3-2	0.002	0.002	0.003	0.007
K1-3	1.374	3.538	6.272	11.429	LR1-3	0.000	0.000	0.000	0.000	LR3-3	0.002	0.002	0.006	0.013
K2-2	0.006	0.009	0.013	0.051	LR1-4	0.000	0.000	0.001	0.002	LR4-2	0.001	0.001	0.001	0.001
K2-3	0.005	0.009	0.013	0.061	LR2-1	6.325				LR4-3	0.002	0.002	0.001	0.001
K3-2	0.103	0.331	0.723	1.884	LR2-3	4.975				K7-2	0.012	0.013	0.036	0.239
K3-3	0.209	0.810	1.627	3.463	LR5-2	0.001	0.001	0.002	0.002	K7-4	0.004	0.005	0.009	0.020
K4-2	8.384	14.436			LR5-3	0.001	0.001	0.002	0.002	K8-2	0.013	0.021	0.037	0.053
K4-3	0.755	0.918	1.524	4.223	K5-2	0.004	0.012	0.023	0.036	K8-3	0.017	0.042	0.155	0.268
K4-4	0.106	0.304	0.854	3.061	K5-3	0.002	0.003	0.004	0.006	K9-2	0.008	0.012	0.030	0.057
K13-1	4.065	6.123	7.964	17.722	K6-1		0.707	1.423		K9-3	0.004	0.008	0.033	0.070
K14-1	3.825	6.162	8.587	13.824	K6-3	0.929	8.802			K10-3	1.675	3.342	6.863	11.392
LS5-2	0.347	1.540	3.227	5.747	K11-2	0.002	0.004	0.005	0.007	K10-4	0.856	1.882	4.691	8.067
LS5-3	0.191	0.937	2.011	6.105	K11-3	0.003	0.005	0.010	0.016	BSF1-2	0.001	0.001	0.012	0.074
LS9-1	0.807	1.970	3.465	5.930	K12-3	1.239	4.307			BSF1-3	0.002	0.003	0.004	0.007
LS9-2	0.666	1.525	2.605	5.000	K12-4	2.878	10.131			BSF1-4	0.002	0.002	0.001	0.002
K16-4	0.083	0.211	0.360	0.609	LS1-2	0.002	0.005	0.018	0.030	BSF2-2	0.000	0.000	0.001	0.001
K16-5	0.010	0.018	0.032	0.067	LS1-3	0.003	0.008	0.036	0.063	BSF2F-2	0.000	0.000	0.000	0.000
K16-6	0.008	0.012	0.019	0.036	LS2-2	5.651				BSF3-2	0.000	0.000	0.000	0.001
K16-1	5.320	9.739			LS2-3	2.727				BSF4-2	0.000	0.000	0.000	0.000
K16-2	7.442	13.681			LS3-2	0.024	0.032	0.040	0.059	BSF4-3	0.000	0.000	0.000	0.000
K16-3	5.996	11.496			LS3-3	0.003	0.017	0.030	0.085	K7-1	0.001	0.001	0.003	0.006
					LS4-2	5.945	12.969			K7-2	0.100	0.270	1.291	2.824
					LS4-3	3.893	8.578	16.043		K7-3	0.024	0.033	0.052	0.076
					LS8-2	0.031	0.079	0.341	1.612	K7-4	0.005	0.012	0.095	0.225
					K15-1	0.001	0.004	0.018	0.031					
					K15-2	0.001	0.002	0.006	0.010					
					K15-3	0.001	0.001	0.005	0.009					
					K15-4	0.027	0.096	0.444	0.792					
					K15-5	0.027	0.091	0.409	0.728					
					K15-6	0.010	0.035	0.158	0.282					
					K11-1	0.004	0.007	0.010	0.013					
					K11-2	0.000	0.001	0.002	0.002					
					K11-3	0.000	0.001	0.002	0.003					
					K6-1	0.032	0.120	0.243	0.329					
					K6-2	0.006	0.013	0.041	0.165					
					K6-3	0.006	0.011	0.028	0.101					

Yellow box = disturbed sites. 0.5 0.6 0.7 0.8 reflect shear velocity values.

REFRENCES

Ashley, W. S., Strader, S., Dziubla, D. C., & Haberlie, A. (2015). Driving blind: Weather-related vision hazards and fatal motor vehicle crashes. *Bulletin of the American Meteorological Society*, *96*(5), 755–778. https://doi.org/10.1175/bams-d-14-00026.1

Bacon, S. N., McDonald, E. V., Amit, R., Enzel, Y., & Crouvi, O. (2011). Total suspended particulate matter emissions at high friction velocities from desert landforms. *Journal of Geophysical Research*, *116*(F3). https://doi.org/10.1029/2011jf001965

Bagnold, R.A., (1941). The Physics of Blown Sand and Desert Dunes. Chapman and Hall, London, p. 265.

Belnap, J. (2003), The world at your feet: desert biological soil crusts. Frontiers in Ecology and the Environment, 1: 181-189. https://doi.org/10.1890/1540-9295(2003)001[0181:TWAYFD]2.0.CO;2

Bowen, B. B., Bernau, J., Kipnis, E. L., Lerback, J., Wetterlin, L., & Kleba, B. (2018). The making of a perfect racetrack at the Bonneville Salt Flats. *The Sedimentary Record*, *16* (2), 4–11. https://doi.org/10.2110/sedred.2018.2.4

Cornelis, W. M., Gabriels, D., & Hartmann, R. (2004). A parameterization for the threshold shear velocity to initiate deflation of dry and wet sediment. *Geomorphology*, *59*(1–4), 43–51. https://doi.org/10.1016/j.geomorph.2003.09.004

Duniway, M. C., Pfennigwerth, A. A., Fick, S. E., Nauman, T. W., Belnap, J., & Barger, N. N. (2019). Wind erosion and dust from US drylands: A review of causes, consequences, and solutions in a changing world. *Ecosphere*, *10*(3). https://doi.org/10.1002/ecs2.2650

Etyemezian, V., Nikolich, G., Ahonen, S., Pitchford, M., Sweeney, M., Purcell, R., Gillies, J., & Kuhns, H. (2007). The portable in situ Wind Erosion Laboratory (PI-SWERL): A new method to measure PM10 windblown dust properties and potential for emissions. *Atmospheric Environment*, *41*(18), 3789–3796. https://doi.org/10.1016/j.atmosenv.2007.01.018

Etyemezian, V., Gillies, J. A., Shinoda, M., Nikolich, G., King, J., & Bardis, A. R. (2014). Accounting for surface roughness on measurements conducted with PI-SWERL: Evaluation of a subjective visual approach and a photogrammetric technique. *Aeolian Research*, *13*, 35–50. https://doi.org/10.1016/j.aeolia.2014.03.002

Gillies, J. A., Furtak-Cole, E., Nikolich, G., & Etyemezian, V. (2022). The role of off-highway vehicle activity in augmenting dust emissions at the Oceano Dunes State

Vehicular Recreation Area, Oceano, CA. *Atmospheric Environment: X*, *13*, 100146. https://doi.org/10.1016/j.aeaoa.2021.100146

Goossens, D., Buck, B., & McLaurin, B. (2012). Contributions to atmospheric dust production of natural and anthropogenic emissions in a recreational area designated for off-road vehicular activity (Nellis Dunes, Nevada, USA). *Journal of Arid Environments*, *78*, 80–99. https://doi.org/10.1016/j.jaridenv.2011.10.015

Goossens, D., & Buck, B. (2009). Dust Dynamics in off-road vehicle trails: Measurements on 16 arid soil types, Nevada, USA. *Journal of Environmental Management*, *90*(11), 3458–3469. https://doi.org/10.1016/j.jenvman.2009.05.031

Goossens, D. (2004). Effect of soil crusting on the emission and transport of wind-eroded sediment: Field measurements on loamy sandy soil. *Geomorphology*, *58*(1–4), 145–160. https://doi.org/10.1016/s0169-555x(03)00229-0

Hartshorn, E. J. (2023). Integrating Sub-Centimeter Resolution Photogrammetry with a Surface Roughness Correction Factor Applied to PI-SWERL Measurements. Retrieved from http://hdl.handle.net/11714/10845

Hahnenberger, M., & Nicoll, K. (2012). Meteorological characteristics of dust storm events in the Eastern Great Basin of Utah, U.S.A. *Atmospheric Environment*, *60*, 601–612. https://doi.org/10.1016/j.atmosenv.2012.06.029

Hahnenberger, M., & Nicoll, K. (2014). Geomorphic and land cover identification of dust sources in the Eastern Great Basin of Utah, U.S.A. *Geomorphology*, *204*, 657–672. https://doi.org/10.1016/j.geomorph.2013.09.013

Hesp, P., Schmutz, P., Martinez, M. L., Driskell, L., Orgera, R., Renken, K., Revelo, N. A., & Orocio, O. A. (2010). The effect on coastal vegetation of trampling on a parabolic dune. *Aeolian Research*, *2*(2–3), 105–111. https://doi.org/10.1016/j.aeolia.2010.03.001

Konert, M., & Vandenberghe, J. (1997). Comparison of laser grain size analysis with pipette and sieve analysis: A solution for the underestimation of the clay fraction. *Sedimentology*, *44*(3), 523–535. https://doi.org/10.1046/j.1365-3091.1997.d01-38.x

Lang, O. I., Mallia, D., & Skiles, M. (2023). The shrinking Great Salt Lake contributes to record high dust-on-snow deposition in the Wasatch Mountains during the 2022 snowmelt season. *Environmental Research Letters*, *18*(6), 064045. https://doi.org/10.1088/1748-9326/acd409

Li, J., Okin, G. S., Herrick, J. E., Belnap, J., Munson, S. M., & Miller, M. E. (2010). A simple method to estimate threshold friction velocity of wind erosion in the field. *Geophysical Research Letters*, *37*(10). https://doi.org/10.1029/2010gl043245

Maddox, N. (2012). Health implications of dust. *CSA News*, *57*(12) 4–9. https://doi.org/10.1002/j.2325-3584.2012.tb02739.x

Mason, J. A., Greene, R. S. B., & Joeckel, R. M. (2011). Laser diffraction analysis of the disintegration of aeolian sedimentary aggregates in water. *CATENA*, *87*(1), 107–118. https://doi.org/10.1016/j.catena.2011.05.015

McLaurin, B., Goossens, D., & Buck, B. (2011). Combining surface mapping and process data to assess, predict, and manage dust emissions from natural and disturbed land surfaces. *Geosphere*, *7*(1), 260–275. https://doi.org/10.1130/ges00593.1

Merrill, T. K. (2023). A Method For Assessing the Effects of Soil Moisture On Dust Emission From Playas and Other Non-Vegetated Surfaces: PI-SWERL Evidence from Great Salt Lake Playa. (Order No. 30524317). Available from ProQuest Dissertations & Theses Global. (2875738334). Retrieved from https://usd.idm.oclc.org/login?url=https://www.proquest.com/dissertations-theses/method-assessing-effects-soil-moisture-on-dust/docview/2875738334/se-2

Middleton, N. J. (2017). Desert dust hazards: A global review. *Aeolian Research*, *24*, 53–63. https://doi.org/10.1016/j.aeolia.2016.12.001

Nauman, T. W., Duniway, M. C., Webb, N. P., & Belnap, J. (2018). Elevated aeolian sediment transport on the Colorado Plateau, USA: The role of grazing, vehicle disturbance, and increasing aridity. *Earth Surface Processes and Landforms*, *43*(14), 2897–2914. https://doi.org/10.1002/esp.4457

Nicoll, K., Hahnenberger, M., & Goldstein, H. L. (2020). 'Dust in the wind' from source-to-sink: Analysis of the 14–15 April 2015 storm in Utah. *Aeolian Research*, *46*, 100532. https://doi.org/10.1016/j.aeolia.2019.06.002

Painter, T. H., Deems, J. S., Belnap, J., Hamlet, A. F., Landry, C. C., & Udall, B. (2010). Response of Colorado River runoff to dust radiative forcing in snow. *Proceedings of the National Academy of Sciences*, *107*(40), 17125–17130. https://doi.org/10.1073/pnas.0913139107

Rodriguez-Caballero, E., Stanelle, T., Egerer, S., Cheng, Y., Su, H., Canton, Y., Belnap, J., Andreae, M. O., Tegen, I., Reick, C. H., Pöschl, U., & Weber, B. (2022). Global cycling and climate effects of aeolian dust controlled by biological soil crusts. *Nature Geoscience*, *15*(6), 458–463. https://doi.org/10.1038/s41561-022-00942-1

Schoenberger, P.J., Momose, T., Wagner, B., Leong, W. H., & Tarnawski, V. R. (2012). Canadian field soils I. Mineral composition by XRD/XRF Measurements. *International Journal of Thermophysics*, *33*(2), 342–362. https://doi.org/10.1007/s10765-011-1142-4

Schoenberger, P.J., Wysocki, D.A., Benham, E.C., and Broderson, W.D. 1998. Field book for describing and sampling soils. Natural Resources Conservation Service, USDA, National Soil Survey center, Lincoln, NE.

Shao, Y., & Klose, M. (2016). A note on the stochastic nature of particle cohesive force and implications to threshold friction velocity for aerodynamic dust entrainment. Aeolian Research, 22, 123–125. https://doi.org/10.1016/j.aeolia.2016.08.004

Smith, J., Burr, S., Reiter, D., & Zeitlin, J. (2009). Recreational off-highway vehicle use on public lands within Utah. *Utah State University Extension*.

Sweeney, M. R. (2022). Dust Emission Processes. *Treatise on Geomorphology*, *7*, 235–258. https://doi.org/10.1016/b978-0-12-818234-5.00015-8

Sweeney, M. R., Lacey, T., & Forman, S. L. (2023). The role of abrasion and resident fines in dust production from Aeolian Sands as measured by the Portable in situ Wind Erosion Laboratory (PI-SWERL). *Aeolian Research*, *63–65*, 100889. https://doi.org/10.1016/j.aeolia.2023.100889

Sweeney, M. R., McDonald, E. V., & Etyemezian, V. (2011). Quantifying dust emissions from desert landforms, eastern Mojave Desert, USA. *Geomorphology*, *135*(1–2), 21–34. https://doi.org/10.1016/j.geomorph.2011.07.022

Whalley, W.B., Marshall, J.R., Smith, B.J., 1982. Origin of desert loess from some experimental observations. Nature 300, 433–435.

Whalley, W.B., Smith, B.J., McAlister, J.J., Edwards, A., 1987. Aeolian abrasion of quartz particles and the production of silt-sized fragments, preliminary results and some possible implications for loess and silcrete formation. In: Reid, I., Frostick, L. (Eds.), Desert Sediments Ancient and Modern. Blackwell, Oxford, pp. 129–138

Webb, N. P., & Pierre, C. (2018). Quantifying anthropogenic dust emissions. *Earth's Future*, *6*(2), 286–295. https://doi.org/10.1002/2017ef000766